

# Resonant-pattern formation induced by additive noise in periodically forced reaction-diffusion systems

Hongli Wang, Ke Zhang, and Qi Ouyang\*

*Department of Physics, Peking University, Beijing 100871, People's Republic of China*

(Received 24 June 2006; revised manuscript received 16 August 2006; published 25 September 2006)

We report frequency-locked resonant patterns induced by additive noise in periodically forced reaction-diffusion Brusselator model. In the regime of 2:1 frequency-locking and homogeneous oscillation, the introduction of additive noise, which is colored in time and white in space, generates and sustains resonant patterns of hexagons, stripes, and labyrinths which oscillate at half of the forcing frequency. Both the noise strength and the correlation time control the pattern formation. The system transits from homogeneous to hexagons, stripes, and to labyrinths successively as the noise strength is adjusted. Good frequency-locked patterns are only sustained by the colored noise and a finite time correlation is necessary. At the limit of white noise with zero temporal correlation, irregular patterns which are only nearly resonant come out as the noise strength is adjusted. The phenomenon induced by colored noise in the forced reaction-diffusion system is demonstrated to correspond to noise-induced Turing instability in the corresponding forced complex Ginzburg-Landau equation.

DOI: [10.1103/PhysRevE.74.036210](https://doi.org/10.1103/PhysRevE.74.036210)

PACS number(s): 05.45.-a, 82.40.Ck, 47.54.-r

## I. INTRODUCTION

It is widely accepted nowadays that noise can play constructive roles and leads to a rich variety of dynamical effects. Far from being a nuisance to be avoided, noise can induce organized and counterintuitive dynamical behavior. Well-known examples in zero-dimensional systems are noise-induced transitions [1] and stochastic resonance [2]. More recently, effects of noise in spatially distributed systems [3] include noise-induced phase transitions [4], noise-induced pattern formation [5], noise-induced fronts [6], and wave nucleation [7], to name only a few. In these and other noise-related phenomena, multiplicative noise, which is coupled to the system state, plays a very special role. However, prominent effect has been also found for additive noise. Such influence has been observed in noise-induced phase transition [8] and pattern formation [9,10], in self-replicating patterns controlled by additive noise [11], and noise-induced front propagation [12]. A recent report [13] demonstrated that additive noise which globally alternates two different monostable excitable dynamics yields pattern formation. In this paper, we report resonant patterns induced by additive noise in oscillatory reaction-diffusion systems subject to periodic forcing.

Oscillatory spatial patterns can conventionally be generated by forcing a spatially extended system. They can be obtained by forcing periodically a system which is autonomously oscillatory [14–23]. This has been studied extensively in both theory and experiment. Similar to that in a single forced nonlinear oscillator, frequency locking occurs in resonantly forced oscillatory reaction-diffusion systems. The entrained system has  $n$ -phase patterns with phases separated by multiples of  $2\pi/n$ , and thus traveling waves are stabilized to standing wave patterns. Resonant patterns such as entrained multiphase oscillating clusters and labyrinthine

standing-wave patterns have been observed in the forced photosensitive Belousov-Zhabotinsky reaction [20–22]. While previous works have studied resonant pattern formation in this type of media, we here focus on the effect of noise and report the phenomenon of noise-induced resonant patterns. It has been recently reported that resonant patterns can also be induced by global periodic switching between two dynamics which are both spatially homogeneous [24]. Our finding lies in that the resonant patterns are generated in the forced oscillatory media and particularly are induced by additive noise which is colored.

The effect of noise on resonant pattern formation in forced oscillatory systems has not been studied until recently [25]. Zhou *et al.* demonstrated with the FitzHugh-Nagumo model that additive noise can affect the frequency of entrained oscillating clusters. We here study the effect of noise on resonant pattern formation in the reaction-diffusion Brusselator which is driven globally by a periodic force. We report that frequency-locked resonant patterns of hexagons, stripes, labyrinths can be induced by additive noise which is temporally colored and spatially white. Furthermore, the noise intensity, the correlation time of the noise control the formation and transition of the resonant patterns. The ordered patterns which oscillate at one-half of the forcing frequency, are noise sustained. They disappear and recede to the 2:1 locked homogeneous oscillations when the noise is moved away. The colored noise is necessary in order to generate the resonant patterns that are exactly frequency locked. At the white noise limit of the colored noise, only irregular patterns which are nearly resonant are produced when the noise strength is adjusted.

In the following, we first give the model and method we used, and give a description of the phenomenon. The result is discussed in the formulation of amplitude equation. We demonstrate that the phenomenon induced by noise in the forced reaction-diffusion system corresponds to noise-induced Turing instability in the corresponding forced complex Ginzburg-Landau equation.

---

\*Electronic address: [qi@pku.edu.cn](mailto:qi@pku.edu.cn)

## II. MODEL AND METHODOLOGY

The model we employ is the reaction-diffusion Brusselator which is driven homogeneously by periodic forces on both variables of the activator and the inhibitor,

$$\frac{\partial u}{\partial t} = a - (1 + b)u + [u^2v + \gamma \cos(\omega t)] + \eta(\mathbf{r}, t) + D_u \nabla^2 u, \quad (1)$$

$$\frac{\partial v}{\partial t} = bu - [u^2v + \gamma \cos(\omega t)] + D_v \nabla^2 v. \quad (2)$$

The forcing enters into the system by modulating periodically the cubic reaction rate.  $\eta(\mathbf{r}, t)$  is the noise introduced additively into the system, which is the Ornstein-Uhlenbeck process that obeys the following stochastic partial differential equation:

$$\frac{\partial \eta(\mathbf{r}, t)}{\partial t} = -\frac{1}{\tau} \eta(\mathbf{r}, t) + \frac{1}{\tau} \xi(\mathbf{r}, t), \quad (3)$$

where  $\xi(\mathbf{r}, t)$  is a Gaussian white noise with zero mean and correlation,

$$\langle \xi(\mathbf{r}, t) \xi(\mathbf{r}', t') \rangle = 2\varepsilon \delta(\mathbf{r} - \mathbf{r}') \delta(t - t'). \quad (4)$$

The colored noise  $\eta(\mathbf{r}, t)$ , which is temporally correlated and white in space, satisfies

$$\langle \eta(\mathbf{r}, t) \eta(\mathbf{r}', t') \rangle = \frac{\varepsilon}{\tau} \exp\left(-\frac{|t - t'|}{\tau}\right) \delta(\mathbf{r} - \mathbf{r}'), \quad (5)$$

where  $\tau$  controls the temporal correlation, and  $\varepsilon$  measures the noise intensity.

For the unforced Brusselator, Hopf instability occurs at  $b_c^H = 1 + a^2$ . Homogeneous oscillation comes up when  $b > b_c^H$ . Turing patterns appear when  $b > b_c^T$  [ $b_c^T = (1 + a\sqrt{D_u/D_v})^2$ ] and  $D_v > \frac{D_u a^2}{(\sqrt{1+a^2}-1)^2}$  are both satisfied. The periodically driven Brusselator with spatial diffusion was investigated recently by forcing only the  $u$  variable [26]. When the system lies in the vicinity of both Hopf and Turing instability, rich oscillating patterns were observed. These patterns result from the interaction of Hopf and Turing instability. As in Ref. [27], we here consider the situation when the unforced system lies far away from the Turing instability (we set always  $D_u \gg D_v$ ), and the system is in the regime of self-sustained Hopf oscillation. On a discrete square lattice, the stochastic partial differential equations (1) and (2) are integrated numerically with periodic boundary conditions by applying the finite difference approach of the Heun algorithm [3]. Except when it is explicitly pointed out, we take parameters  $a=2$ ,  $b=5.3$ ,  $\gamma=1.2$ ,  $\omega=4.18$ ,  $D_u=0.2$ ,  $D_v=0.02$  throughout this paper. The noise intensity  $\varepsilon$  and correlation time  $\tau$  are adjusted as control parameters.

## III. RESULTS

When the system is noise free and with the parameter values we take, the forced oscillatory media lies in the re-

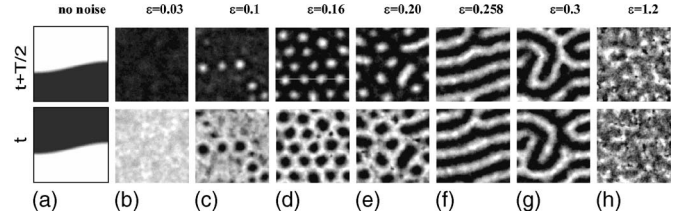


FIG. 1. Frequency-locked patterns including hexagons, stripes, and labyrinths that are induced by colored noises of different strength. The images are grey-scaled snapshots of  $u$  field at an instant  $t$  (bottom), and at one-half oscillation period  $T/2$  (top) later. Noise strength  $\varepsilon$  is increased from 0.03 to 0.1, 0.16, 0.2, 0.258, 0.3, and 1.2 for columns (b), (c), (d), (e), (f), (g), and (h), respectively. Other parameters,  $a=2$ ,  $b=5.3$ ,  $D_u=0.2$ ,  $D_v=0.02$ ,  $\omega=4.18$ ,  $\gamma=1.2$ . Noise correlation time  $\tau=0.8$ . The lattice size is  $128 \times 128$  with spacing 0.25. The initial condition for the noise-induced patterns is the randomly perturbed homogeneous equilibrium ( $u=a$ ,  $v=b/a$ ).

gime of 2:1 frequency locking. The system oscillates at one-half of the forcing frequency. Dependent on the initial conditions, two-phase patterns, with a phase shift of  $\pi$  and separated by a stationary Ising front, appear [Fig. 1(a)], or alternatively homogeneous oscillations come out. From the random initial condition prepared by randomly perturbing the homogeneous steady state  $u=a$ ,  $v=b/a$ , we obtain 2:1 resonant homogeneous oscillations.

We turn on the additive noise and adjust the noise strength and correlation length to check their effects on the homogeneous oscillation. At a first series of simulations, we adopt  $\tau=0.8$ , and adjust the noise intensity  $\varepsilon$ . When  $\varepsilon$  is small, the homogeneous oscillation is only slightly perturbed by the noise as depicted in Fig. 1(b). As  $\varepsilon$  is increased, the homogeneous oscillating pattern loses its stability. Figure 1(c) shows that oscillating two-phase pattern with bubbles appear at  $\varepsilon=0.1$ . When the noise strength is increased, the bubbled pattern becomes more and more regular. At  $\varepsilon=0.16$ , clear oscillating hexagonal pattern is generated [Fig. 1(d)]. As the noise strength grows to even larger values, the hexagonal pattern loses its stability again. Figure 1(e) demonstrates that the hexagons merge and form a mixed pattern of hexagons and stripes. The hexagons transit to stripes at  $\varepsilon=0.258$  [Fig. 1(f)]. At  $\varepsilon=0.3$ , the stripes are unstable, and labyrinths dominate as seen in Fig. 1(g). At sufficiently large  $\varepsilon$ , the pattern becomes irregular [Fig. 1(h)]. The ordered pattern is finally destroyed by the noise. All these patterns are noise sustained. They disappear and resort to the original homogeneous oscillations after the noise is turned off. The patterns [Figs. 1(c)–1(g)] induced by the noise are resonantly locked. They are standing waves that oscillate at half of the driving frequency. As an example shown in Fig. 2, the space-time plot for the hexagonal pattern of Fig. 1(d) in comparison with the external forcing amplitude illustrates that the patterns are well 2:1 frequency locked.

Spatial Fourier transformation of the hexagonal pattern in Fig. 1(d) reveals that the pattern which is temporally resonant is also in spatial resonance. Figure 3(a) depicts that the wave vectors of spatial Fourier transformation form a hexagon which is typical for hexagonal Turing patterns.

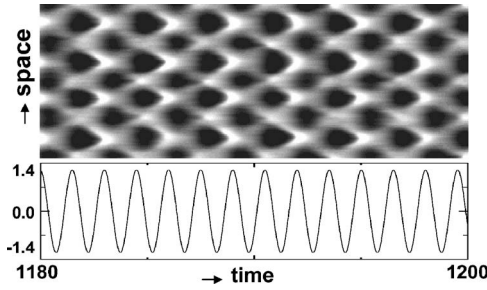


FIG. 2. Space-time diagram (top panel, with vertical space and horizontal time) displaying the time evolution of the pattern along the cross section marked in the two-dimensional image of Fig. 1(d). For comparison, the curve at the bottom shows the periodic external forcing. The pattern oscillates at one-half of the external forcing frequency demonstrating a 2:1 frequency locking.

In previous experiments or simulations, the labyrinthine patterns have been found to be ample and easily observed in periodically forced self-sustained oscillating media. The resonant hexagonal pattern was predicted in this type of media by the forced amplitude equation [15], but has rarely been found in experiments or simulations. Hexagonal patterns appear most frequently in systems undergoing a Turing instability. It was reported that hexagonal patterns that oscillate can be generated from the interaction between a Turing mode and Hopf oscillation in either periodically forced [26] or unforced [28,29] reaction-diffusion systems. The patterns thus produced are termed as oscillating Turing patterns which are phenomenologically very similar to those we find here. The resonant hexagons in Fig. 1(d) were however generated with parameters far away from the regime of Turing bifurcation (we set  $D_u \gg D_v$ ). Furthermore, the patterns we obtain are strictly standing waves which are stable in space,

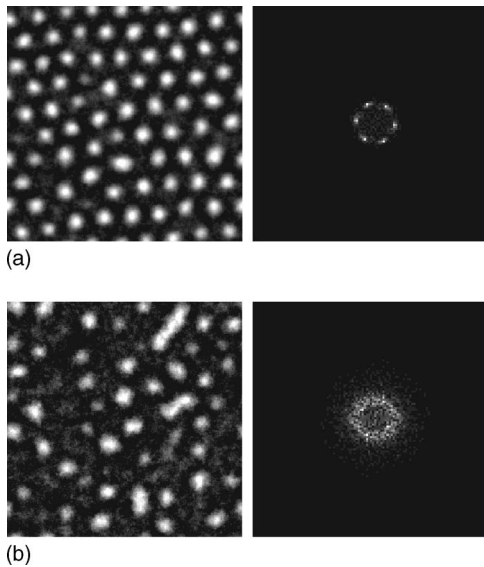


FIG. 3. Patterns (left-hand column) and their spatial Fourier transformation (right-hand column). The resonant hexagonal pattern of (a) is computed with parameters as in Fig. 1(d); the pattern of (b) is obtained under the influence of white noise with intensity  $\varepsilon = 0.12$ .  $256 \times 256$  lattice is used for generating the patterns.

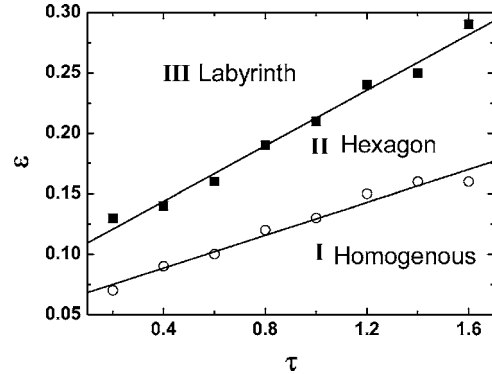


FIG. 4. Phase diagram in  $\varepsilon$ - $\tau$  parameter space.

while the oscillating Turing patterns drifted slightly in space as reported in Ref. [26]. The oscillatory spatial patterns reported here are similar to those found in Ref. [24], where resonant hexagonal patterns were generated by switching periodically between two spatially homogeneous stable states. The difference of our results lies in that the resonant patterns are generated in the forced oscillatory media which are induced by additive colored noise.

The role of temporal correlation  $\tau$  of the noise is significant in inducing and controlling the formation and transition of the resonant patterns. As  $\tau$  is increased, a larger value of noise strength  $\varepsilon$  is required in order to generate the patterns than otherwise with a smaller  $\tau$ . We scanned the correlation time and noise strength, and generated  $\tau$ - $\varepsilon$  phase diagram. Figure 4 depicts that the transition point is shifted toward higher values of the noise intensity as the correlation time is increased, that is,  $\tau$  softens the effect of the noise. The softening effect [30] of the correlation time is obvious from the definition of noise  $\eta$ . In Eqs. (3) and (5), an increase in  $\tau$  tends to weaken the effective noise intensity, and a pattern obtained with a relatively smaller  $\tau$  therefore needs a larger value of  $\varepsilon$  when  $\tau$  is increased. As  $\tau$  goes to infinity, the Ornstein-Uhlenbeck process goes to a no-noise limit. In this case, noise-free behavior, that is homogeneous oscillations in this context, should be recovered. Figure 5 demonstrates the effect of growth in  $\tau$  on the hexagonal pattern shown in Fig. 1(d). As  $\tau$  increases to 1.4 and 2.0, the system recedes to bubbled patterns as that shown in Fig. 1(c). At  $\tau = 10.0$  [Fig. 5(d)], the patterns are approximately homogeneous as in Fig. 1(b).

At the other limit of the colored noise,  $\tau$  goes to zero and white noise is obtained. In this limit, the forced system is no

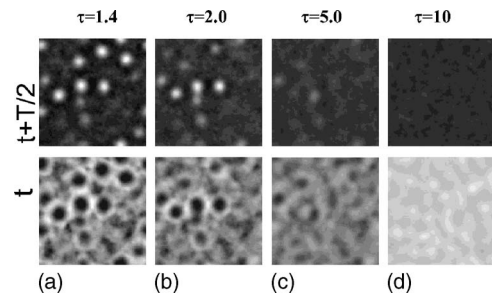


FIG. 5. Effect of correlation time  $\tau$  of noise  $\eta$ :  $\tau = 1.4$  for (a), 2 for (b), 5 for (c), and 10 for (d). Other parameters are as Fig. 1(d).

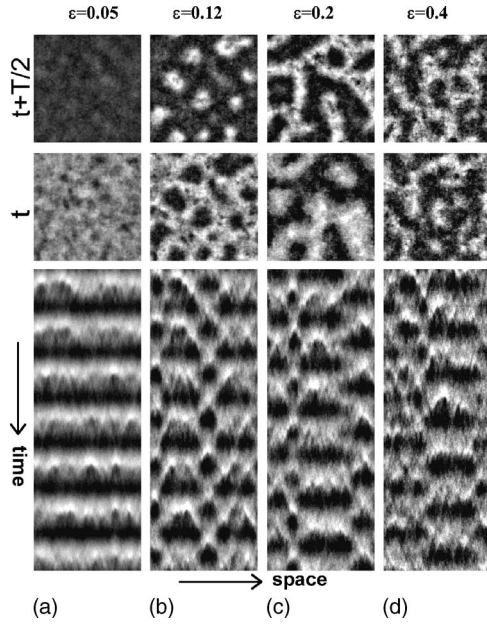


FIG. 6. Effect of white noise with different intensities. The top two rows are snapshots taken at time  $t$  and  $t+T/2$ , respectively. The bottom panels are space-time diagrams displaying the time evolutions of the nearly resonant patterns, which are generated as that in Fig. 2. Parameters:  $\varepsilon=0.05$  for column (a), 0.12 for column (b), 0.2 for column (c), and 0.4 for column (d). Other parameters are the same as Fig. 1.

longer completely frequency locked as the noise strength is scanned. The noise sustains only irregular patterns that are only approximately resonant. This is true in the whole parameter ranges that we have checked. Figure 6 depicts the patterns and their time evolutions when  $\varepsilon$  grows from 0.05 to 0.12, 0.2, and 0.4. Irregular spotted patterns [Fig. 6(b)] and labyrinths [Fig. 6(c)] are generated. The space-time diagrams depict that the patterns do not repeat themselves exactly after a time period of  $T$ . This is in contrast with the case shown in Fig. 2 where the resonant pattern is sustained by colored noise. Figure 6(b) are apparently similar to hexagons shown in Fig. 1(d). But as compared in Fig. 3, the pattern sustained by white noise [Fig. 3(b)] do not have as good space periodicity as the pattern sustained by colored noise [Fig. 3(a)]. Our numerical simulations indicate that the colored noise is the source of good resonance, and nonzero  $\tau$  is necessary in order to maintain good frequency-locked patterns such as hexagons, stripes, and labyrinths.

We adopt a simple intensive order parameter to characterize transitions between resonant patterns which are controlled by  $\tau$  and  $\varepsilon$ . It is defined as

$$m = \frac{\sum_{i,j} u_{i,j}}{N^2}, \quad (6)$$

where  $N$  is the lattice size,  $u_{i,j}$  is the concentration of  $u$  variable at a discrete site  $(i,j)$ . Due to that the patterns are time dependent, the sum is calculated at the instant when  $\cos(\omega t/2) = -1$ , and  $m$  is obtained as the mean of many times of calculations. Figure 7 displays the dependence of the order parameter  $m$  on the noise intensity  $\varepsilon$ . The curves are

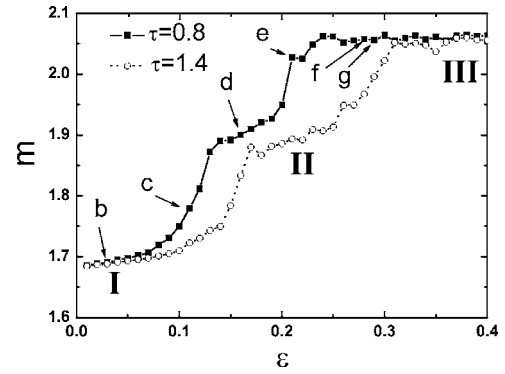


FIG. 7. Order parameter  $m$  vs  $\varepsilon$  with correlation time  $\tau=0.8$  (squares), and  $\tau=1.4$  (circles). The arrow-marked points correspond to frequency-locked patterns in Figs. 1(b)–1(g), respectively. I, II, and III denote the locked patterns of homogeneity, hexagon, and stripes or labyrinth, respectively.

calculated by increasing  $\varepsilon$  continuously, and at each value of  $\varepsilon$  the order parameter  $m$  is calculated after sufficient long time of evolution. As shown in Fig. 7,  $m$  grows in a step-up manner. The stages of planar growth correspond to homogeneous oscillations (I), resonant hexagonal patterns (II), and stripes or labyrinthine patterns (III), respectively. At the transition stages, the resonant patterns change drastically and  $m$  grows rapidly as  $\varepsilon$  increases. The softening effect of the noise correlation time is also manifested in Fig. 7. The transition points are shifted toward higher values of noise intensity.

#### IV. DISCUSSIONS

To explore the effect of noise, the linear analysis of stability with the help of Novikov's theorem [31] which is applicable for multiplicative noise is not directly usable for the additive noise. One must resort to the approach of structure functions within linear approximation and the mean field approach [3], or adopt the recent moment-based analysis [10]. As the system we consider here is subject to periodic forcing and involves resonant patterns, the conventional approaches are not directly applicable. In the following, we consider the amplitude equation for resonantly forced oscillatory systems, and show that the noise-induced resonant patterns in the forced reaction-diffusion Brusselator correspond to the noise-induced Turing instabilities in the forced complex Ginzburg-Landau equation (CGLE).

As has been demonstrated in previous experiments and simulations, the above resonant patterns induced by noise appear conventionally in forced oscillatory media that are not influenced by noise, and are analyzed in the formulation of the forced CGLE [15]. It has the following form:

$$\frac{\partial A}{\partial t} = (\mu + i\nu)A - (\alpha_r + i\alpha_i)|A|^2A + (\beta_r + i\beta_i)\nabla^2 A + \bar{\gamma}A^{n-1}, \quad (7)$$

The parameters in the equation are related to those in the Brusselator model:  $\mu = \frac{b-b_c}{2}$ ,  $\nu = w_0 - w/2$ ;  $\alpha_r = 1/a^2 + 1/2$ ,  $\alpha_i$

$$= \frac{2}{3a^2} - \frac{7}{6a} + \frac{2a}{3}; \quad \beta_r = (D_u + D_v)/2, \quad \beta_i = a(D_v - D_u)/2; \quad \tilde{\gamma} = \frac{\gamma^2 4a^4 - 11a^2 + 4}{6a^2}.$$
 Variable  $A$  is the complex amplitude of the resulting nonlinear oscillations with period  $T = 2\pi n/w$ . Equation (7) describes a spatially extended oscillatory system subject to resonant periodic forcing at frequency  $w \approx n\omega_0$ , where  $\omega_0$  is the natural frequency of the unforced spatially homogeneous oscillations. A theoretical study [15] of the above equation showed that resonant forcing can exhibit rich patterns as the external frequency is varied. We consider 2:1 resonance by taking  $n=2$  in accordance with our simulations, and concentrate on the effect of noise in the forced CGLE.

By introducing additively the noise  $\eta(\mathbf{r}, t)$  of Eq. (3) into Eq. (7), we generate spatially stationary patterns similar to the noise-induced Faraday-type patterns in Fig. 1. In Eq. (7), there are two symmetrical homogeneous steady states (HSS)  $A_0$ , and  $-A_0$ , together with the equilibrium  $(0, 0)$  which is unstable. In the original forced reaction-diffusion equations, the bistable HSS states  $A_0$  and  $-A_0$  correspond to the entrained oscillations of opposite phases. As the noise  $\eta$  is added to Eq. (7), we find that Turing bifurcations can be induced and occur on both branches of the symmetrical HSS states. When  $\varepsilon$  and  $\tau$  are adjusted, we observe similar scenario of phase transitions to that shown in Fig. 1. Figure 8 demonstrates that the homogeneous steady states become unstable as the noise intensity is increased, and patterns of hexagons [Fig. 8(b)] and labyrinths [Fig. 8(d)] are successively induced. In Fig. 8, top and bottom panels are patterns evolving from the instabilities of  $A_0$  and  $-A_0$ , respectively. This indicates that the Turing patterns in Figs. 8(b)–8(d) induced by noise in the forced CGLE correspond to the resonant 2:1 patterns generated in Eqs. (1) and (2).

The Turing patterns in Fig. 8 are induced when the noise is weak. As the noise intensity is increased, Turing patterns bifurcated from  $A_0$  and  $-A_0$  will be ruined. The labyrinthine patterns are not spatially stationary with  $\varepsilon=0.15$  [Fig. 8(e)]. The patterns are destroyed completely when the noise strength is sufficiently large with  $\varepsilon=0.5$  [Fig. 8(f)].

It has been reported that additive noise can significantly shift the boundaries of phase transitions in nonlinear chains

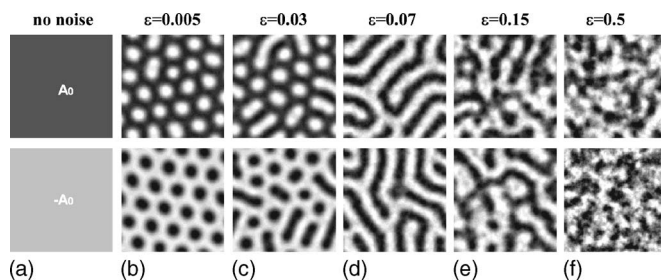


FIG. 8. Stationary Turing patterns (b), (c), and (d) coded in the grey scale of the real part of  $A$  in the forced CGLE induced by noises of different strength  $\varepsilon$ . The top and bottom panels correspond to the patterns induced by the noise from the bistable states of  $A_0$  [(a) top] and  $-A_0$  [(a) bottom], respectively. Parameters in Eq. (7):  $\tau=0.8$ ,  $\mu=0.15$ ,  $\nu=-0.115$ ,  $\alpha_r=0.75$ ,  $\alpha_i=5/6$ ,  $\beta_r=0.11$ ,  $\beta_i=-0.18$ ,  $\gamma=0.245$ , which correspond to parameters  $a=2$ ,  $b=5.3$ ,  $D_u=0.2$ ,  $D_v=0.02$ ,  $w=4.23$ ,  $\gamma=1.2$  in Eqs. (1) and (2). The HSS state  $A_0 = (-0.229\ 26, 0.282\ 73i)$ . The initial condition for top and bottom panels is  $A_0$  and  $-A_0$ , respectively.

induced by multiplicative noise [32], or in the conserved Ginzburg-Landau model [30]. The phenomenon of additive-noise-induced resonant patterns we demonstrated here presents another example of significant effects of additive noise. Numerical exploration of Eqs. (1) and (2) that are not influenced by the noise  $\eta(\mathbf{r}, t)$  showed that resonant patterns induced by the colored noises can be generated by adjusting the forcing amplitude and frequency. The parameters under which the resonant patterns are generated from Eqs. (1) and (2) turn out to lie in the vicinity of the transition boundaries. The effect of the noise on the forced Brusselator or on the forced CGLE lies in that it shifted the transition boundaries and advanced the appearance of phase transitions.

#### ACKNOWLEDGMENT

The work is supported by the National Natural Science Foundation of China.

- 
- [1] W. Horsthemke and R. Lefever, *Noise-Induced Transitions* (Springer, Berlin, 1984).
- [2] L. Gammaitoni, P. Hanggi, P. Jung, and F. Marchesoni, *Rev. Mod. Phys.* **70**, 223 (1998).
- [3] J. García-Ojalvo and J. M. Sancho, *Noise in Spatially Extended Systems* (Springer, New York, 1999).
- [4] C. Van den Broeck, J. M. R. Parrondo, and R. Toral, *Phys. Rev. Lett.* **73**, 3395 (1994); C. Van den Broeck, J. M. R. Parrondo, R. Toral, and R. Kawai, *Phys. Rev. E* **55**, 4084 (1997); S. Mangioni, R. Deza, H. S. Wio, and R. Toral, *Phys. Rev. Lett.* **79**, 2389 (1997); S. Mangioni, R. R. Deza, R. Toral, and H. S. Wio, *Phys. Rev. E* **61**, 223 (2000); M. Ibañes, J. Garcia-Ojalvo, R. Toral, and J. M. Sancho, *Phys. Rev. Lett.* **87**, 020601 (2001).
- [5] J. Buceta, M. Ibanes, J. M. Sancho, and K. Lindenberg, *Phys. Rev. E* **67**, 021113 (2003); K. Wood, J. Buceta, and K. Lindenberg, *ibid.* **73**, 022101 (2006).
- [6] M. A. Santos and J. M. Sancho, *Phys. Rev. E* **59**, 98 (1999); L. Q. Zhou, X. Jia, and Q. Ouyang, *Phys. Rev. Lett.* **88**, 138301 (2002).
- [7] P. Jung and G. Mayer-Kress, *Phys. Rev. Lett.* **74**, 2130 (1995); S. Alonso, I. Sendina-Nadal, V. Perez-Munuzuri, J. M. Sancho, and F. Sagues, *ibid.* **87**, 078302 (2001); V. Beato, I. Sendina-Nadal, I. Gerdes, and H. Engel, *Phys. Rev. E* **71**, 035204(R) (2005).
- [8] P. S. Landa, A. A. Zaikin, V. G. Ushakov, and J. Kurths, *Phys. Rev. E* **61**, 4809 (2000); A. Zaikin and J. Kurths, *Chaos* **11**, 570 (2001).
- [9] A. A. Zaikin and L. Schimansky-Geier, *Phys. Rev. E* **58**, 4355 (1998).
- [10] S. S. Riaz, S. Dutta, S. Kar, and D. S. Ray, *Eur. Phys. J. B* **47**, 255 (2005).

- [11] F. Lesmes, D. Hochberg, F. Morán, and J. Pérez-Mercader, *Phys. Rev. Lett.* **91**, 238301 (2003).
- [12] M. G. Clerc, C. Falcon, and E. Tirapegui, *Phys. Rev. Lett.* **94**, 148302 (2005).
- [13] X. Sailer, D. Hennig, V. Beato, H. Engel, and L. Schimansky-Geier, *Phys. Rev. E* **73**, 056209 (2006).
- [14] P. Couillet, J. Lega, B. Houchmanzadeh, and J. Lajzerowicz, *Phys. Rev. Lett.* **65**, 1352 (1990).
- [15] P. Couillet and K. Emilson, *Physica D* **61**, 119 (1992).
- [16] C. Elphick, A. Hagberg, and E. Meron, *Phys. Rev. E* **59**, 5285 (1999).
- [17] H. K. Park, *Phys. Rev. Lett.* **86**, 1130 (2001).
- [18] C. Hemming and R. Kapral, *Physica D* **168**, 10 (2002).
- [19] I. V. Barashenkov and S. R. Woodford, *Phys. Rev. E* **71**, 026613 (2005).
- [20] V. Petrov, Q. Ouyang, and H. L. Swinney, *Nature (London)* **388**, 655 (1997).
- [21] A. L. Lin, M. Bertram, K. Martinez, H. L. Swinney, A. Ardelea, and G. F. Carey, *Phys. Rev. Lett.* **84**, 4240 (2000); A. L. Lin, A. Hagberg, A. Ardelea, M. Bertram, H. L. Swinney, and E. Meron, *Phys. Rev. E* **62**, 3790 (2000); A. L. Lin, A. Hagberg, E. Meron, and H. L. Swinney, *ibid.* **69**, 066217 (2004).
- [22] V. K. Vanag, A. M. Zhabotinsky, and I. R. Epstein, *Phys. Rev. Lett.* **86**, 552 (2001).
- [23] M. Bertram, C. Beta, H. H. Rotermund, and G. Ertl, *J. Phys. Chem. B* **107**, 9610 (2003).
- [24] J. Buceta, K. Lindenberg, and J. M. R. Parrondo, *Phys. Rev. Lett.* **88**, 024103 (2002); J. Buceta and K. Lindenberg, *Phys. Rev. E* **66**, 046202 (2002).
- [25] C. Zhou and J. Kurths, *Phys. Rev. E* **69**, 056210 (2004).
- [26] L. Yang, A. M. Zhabotinsky, and I. R. Epstein, *Phys. Rev. Lett.* **92**, 198303 (2004).
- [27] K. Zhang, H. Wang, C. Qiao, and Q. Ouyang, *Chin. Phys. Lett.* **23**, 1414 (2006).
- [28] A. Rovinsky and M. Menzinger, *Phys. Rev. A* **46**, 6315 (1992).
- [29] L. Yang and I. R. Epstein, *Phys. Rev. Lett.* **90**, 178303 (2003).
- [30] J. García-Ojalvo and J. M. Sancho, *Phys. Rev. E* **49**, 2769 (1994).
- [31] A. Becker and L. Kramer, *Phys. Rev. Lett.* **73**, 955 (1994).
- [32] P. S. Landa, A. A. Zaikin, and L. Schimansky-Geier, *Chaos, Solitons Fractals* **9**, 1367 (1998).